Available online at www.sciencedirect.com
ScienceDirect
Journal of Nuclear Materials 360 (2007) 282–292
journal of nuclear materials
www.elsevier.com/locate/jnucmat

Influence of protecting gel film on oxidation of zirconium alloys

H. Frank [a,*], Z. Weishauptova [b], V. Vrtilkova [c]

[a] Department of Solid State Engineering, Faculty of Nuclear Sciences and Physical Engineering, Czech Technical University, Trojanova 13, 120 00 Prague 2, Czech Republic
[b] Institute of Rock Structure and Mechanics, AVCR, V Holesovickach 41, Prague 8, Czech Republic
[c] UJP Praha a.s., Nad Kaminkou 1345, 156 10 Prague 5, Czech Republic

Received 27 March 2006; accepted 30 October 2006

Abstract

Thin oxide layers of Zr1Nb and Zry-4S on tubes, used for fuel cladding in light water reactors, which had been protected by thin gel films, were compared with oxide layers on unprotected specimens of the same kind, grown together in two batches in water at 360 °C for 21 and 42 days, respectively. The analysis of the *I–V* characteristics at constant temperatures up to 180 °C showed a strong decreasing resistivity with oxidation time of the gel-protected layers of the Zry-4S specimens, with indication of an energy dependent trap distribution, although the gel and the oxide alone showed evidence of single, but different, energy traps. The changes are believed to be due to diffusion of different trap centers in both directions. The Zr1Nb specimens retained their single energy trap behaviour also in the combination with the protecting gel film and resistivity dropping with increasing oxidation time.

1. Introduction

The results presented in this paper were achieved continuing the investigation of the transport properties of oxide layers of zirconium alloys described earlier [1]. Zirconium alloys are being used in nuclear light water reactors as fuel cladding and channel box materials because of their enhanced corrosion resistance [2,3]. In a high-temperature aqueous environment, oxides are formed by diffusion of oxygen ions through the built-up oxide layer, combining with zirconium ionized by electron emission [4]. The corrosion of zirconium is due to oxide formation by the transfer of electrons from the metal to water, with oxygen ions flowing in the opposite direction. The corrosion rate depends largely on the electron motion, which is governed by the electrical conductivity of the oxide layer. The rate of oxide growth depends on the resistance of the already built-up layer, the thicker the layer, the slower it will grow. It is therefore plausible that an artificially applied oxide film will protect the underlying metal, retarding the corrosion, and thus lengthening the utilizable time of the cladding. The investigation of the electrical properties of the oxide, especially of the double layer consisting of the protecting surface layer and the underlying growing oxide layer, is therefore of interest for understanding the mechanism of oxide formation and corrosion resistance. Howlader et al. [4]

* Corresponding author. Tel.: +420 2 2435 8559; fax: +420 2 2191 2407.
E-mail address: frank@km1.fjfi.cvut.cz (H. Frank).

0022-3115/$ - see front matter © 2006 Elsevier B.V. All rights reserved.
doi:10.1016/j.jnucmat.2006.10.013

concluded that electron conduction dominates the electrical conductivity of Zircaloy oxide films. It is well known [4–6] that ZrO_2 is predominantly an electronic high-resistivity semiconductor with a low amount of ionic conduction. The band gap is approximately 5 eV, the work function 4.0 eV and the relative permittivity 22.

2. Samples

Tube specimens 30 mm long and of 9 mm outer diameter prepared from zirconium alloys Zr1Nb and Zry-4S in pairs, with and without applied gel film, had been oxidized in water of 360 °C, the first two pairs for 21 days, and the second two pairs for 42 days. For determination of the properties of the gel layer itself, one tube of Zr1Nb with applied gel was left without oxidation.

The gel films were prepared by sol–gel synthesis. The precursor for the sol was a mixture of isopropoxide Zr(IV) and isobutanole stabilized with 2,2′-diethanolamine, concentration $n(\mathrm{DEA})/n(\mathrm{metal}) = 1$. The viscosity was enhanced by adding polyvinylpyrrolidone (PVP) with a concentration of $n(\mathrm{PVP})/n(\mathrm{metal}) = 0.3\mathrm{max}$ [12,13].

The films were formed in air by dip-coating with a velocity of 3 mm/s on the thoroughly cleaned Zr surface. The samples were dried at first 5 min in air at 403 K and then annealed 15 min in oxygen in a furnace at 400 °C. After cooling to room temperature the coating process was repeated five times. It was observed by Raman spectroscopy that the samples retained their amorphous structure. The thickness of the films was measured by means of a Hommel Tester 1000 type profilometer on smooth silicon surfaces to exclude the influence of surface roughness on the Zr tubes.

The chemical composition of the samples is given in Table 1 and the sample parameters are in Table 2.

Table 1
Chemical composition (wt%) of used zirconium alloys

	Nb	Sn	Fe	Cr
Zr1Nb	1	–	–	–
Zry-4S	–	1.46	0.2	0.1

3. Experimental

Vacuum evaporated gold electrodes 200 nm thick and 6 mm diameter were not satisfactory, as there appeared to be weak spots in the oxide films causing shorts. Therefore painted-on contacts of colloidal silver (Degussa Leitsilber 317) of about 2 mm diameter were used, the smaller contact area having a larger probability of avoiding weak spots. Out of five contacts on a sample at least two were acceptable after annealing in air at 180 °C. The specimens were mounted in a small thermostat with a maximum temperature of 220 °C. The abraded front ends of the tubes of shining zirconium metal were in direct contact with pressed-on copper electrodes, on which a thermocouple was mounted for temperature control. The current was measured with a two-electrode arrangement, using only one contact to each electrode. The contact resistance between the copper electrodes pressed onto the metallic bulk zirconium, being a fraction of an Ohm, compared to the resistance of the samples of the order of $10^9\ \Omega$, is certainly to be neglected, the same being true for the resistance between the silver electrode and the pressed-on 0.3 mm thick phosphorbronze contact spring. A stabilized voltage source could

Table 2
Characterization of the samples

Sample	Short name	Oxidation (days)	Gel	Thickness (μm)	Oxide (μm)	Gel (μm)
T 1936017 Zr1Nb	T-Zr1Nb-1	21	Gel	4.02	2.35	1.67
1936117 Zr1Nb	Zr1Nb-1	21	–	2.81	2.81	–
T 41 (Zr1Nb)	T-41	–	Gel	1.5	–	1.5
T 4936017 Zry-4S	T-Zry-4S-1	21	Gel	3.26	1.48	1.78
4936117 Zry-4S	Zry-4S-1	21	–	1.78	1.78	–
T 1936025 Zr1Nb	T-Zr1Nb-2	42	Gel	4.97	2.98	1.99
1936125 Zr1Nb	Zr1Nb-2	42	–	3.27	3.27	–
T 4936025 Zry-4S	T-Zry-4S-2	42	Gel	2.81	1.5	1.31
4936125 Zry-4S	Zry-4S-2	42	–	1.84	1.84	–

Abbreviated sample names for shortness, T – tetragonal gel, 1, 2 – oxidation 21, 42 days.

be connected with the positive terminal to the zirconium metal contact, while the negative terminal was earthed to the pico-amperemeter common. The input terminal was connected via a contact spring to the silver electrode. The voltage drop of the pico-amperemeter was limited to 10 mV max. and could be neglected for source voltages larger than 2 V.

After painting on, the silver contact was left to dry in air at room temperature for several hours, and was then slowly heated in the thermostat with a rate of about 1 °C/min. The short-circuit current was measured without application of external voltage, and the open-circuit voltage assessed by compensation of the short-circuit current. Readings were taken in steps of 5 °C, up to 180 °C. After the first heating, which served to anneal the silver contact, the same procedure was repeated after cooling down to room temperature and the values of the short-circuit current and open-circuit voltage were used to plot $\log\rho = f(1/T)$ and to compute the activation energy. The observed short-circuit current is due to a continuing oxidation of the zirconium in air at elevated temperatures [1].

Then the capacity was measured with a TESLA BM 498 type capacitance bridge operating at 1000 Hz with a 0.1% precision. Afterwards the *I–V* characteristics were measured, first at room temperature and then at constant higher temperatures from 40 to 180 °C with 20 °C steps. The voltage was applied in steps of 1/10 of the maximum voltage, which was chosen individually for each sample in such a way as to avoid overstraining of the contact, meaning that the space-charge limited current at the maximum voltage was about 10 times higher than the current of the linear, ohmic part. Although there exists a small asymmetry in the complete *I–V* characteristics due to a certain rectifying effect, only the forward voltage branch, with the positive voltage terminal connected to the zirconium metal, was measured. As a consequence of the small thickness of the oxide layers, the injection process was soon terminated, and constant current was reached after a few minutes.

The *I–V* characteristics of high-resistivity semiconductors start at low voltages with a linear part obeying Ohm's law. At application of higher voltages the current rises faster due to the injection of majority carriers building up a space charge. The current develops a space-charge limited additional part. The measured current values can be fitted to a second order polynomial

$$I = aU^2 + bU + c. \tag{1}$$

The zero-current expressed by the constant c can be observed above room temperature as a consequence of temperature-activated liberation of trapped electrons and/or continuing oxidation in air. The space-charge limited current I_{sc}, i.e. the first term in Eq. (1), obeys Child's law [7]

$$I_{sc} = \frac{9}{8}\varepsilon\varepsilon_0 A\mu U^2/w^3 = aU^2, \tag{2}$$

where $\varepsilon\varepsilon_0$ is the relative and vacuum permittivity, respectively, A is the contact area, μ is the mobility of the free carriers, U the applied voltage and w the layer thickness. The transition from the linear to the square part I_{sc} occurs at the characteristical voltage U_{ch}, when the rising space-charge limited current equals the linear ohmic part $I_o = bU$, i.e.

$$AU^2 = bU, \quad \text{or} \quad U = U_{ch} = b/a. \tag{3}$$

The ohmic current is

$$I_o = U/R = Uen_0\mu w/A. \tag{4}$$

The characteristical voltage U_{ch}, using Eqs. (2) and (4), yields

$$U_{ch} = en_0w^2/\varepsilon\varepsilon_0. \tag{5}$$

By this expression the concentration n_0 of the free carriers can be obtained,

$$n_0 = U_{ch}\varepsilon\varepsilon_0/ew^2. \tag{6}$$

This is a simple way to assess the concentration of the free carriers n_0 which, with knowledge of the resistivity ρ measured in the vicinity of the origin, yields also the mobility μ.

An other way to assess the mobility is using Eq. (2) directly.

In the presence of traps with the concentration $N_{t(s)}$ at a single energy level E_s, Eq. (2) is changed to

$$I_{sc} = \frac{9}{8}\varepsilon\varepsilon_0\mu A\frac{N_C}{N_{t(s)}}\exp\left(-\frac{E_s}{kT}\right)\frac{U^2}{w^3}, \tag{7}$$

where N_C is the effective density of states in the conduction band. If the current is measured at a constant voltage as the function of temperature, then plotting $\log I = f(1/T)$ appears as a straight line with the slope yielding the activation energy E_s of the

traps. Measurement of the temperature dependence of the current at various constant voltages yields as many straight lines, which will be parallel, i.e. all having the same slope giving the same activation energy. This indicates that there is only one type of traps at a single energy level $E_{t(s)}$. With traps the characteristical voltage changes to U_F

$$U_F = U_{ch}/\theta, \tag{8}$$

where $\theta = N_C/N_{t(s)} = n/n_t$ is the ratio of free to trapped charge [8]. When the Fermi level E_F rises over the trap level, the traps are flooded and the current rises with a higher power when the voltage exceeds U_F. The concentration of the traps can then be computed using

$$U_F = eN_{t(s)}w^2/\varepsilon\varepsilon_0. \tag{9}$$

Instead of traps on a single energy level there can be traps distributed exponentially below the conduction band edge. For this case Lampert [9] has shown that the space-charge limited current is given by

$$I = e\mu N_C A\left(\frac{\varepsilon\varepsilon_0}{eP_0kT_t}\right)^l \frac{U^{l+1}}{w^{2l+1}}, \tag{10}$$

here P_0 is the trap density per unit energy range at the conduction band edge and l is the ratio T_t/T where T_t is a temperature parameter characterizing the exponential trapping distribution

$$P(E) = P_0 \exp(-E/kT_t), \tag{11}$$

where $P(E)$ is the trap density per unit energy range at an energy E below the conduction band edge. The total trapping concentration N_t is given by Gould and Rahman [10] as

$$N_t = P_0kT_t. \tag{12}$$

On the basis of the above expressions Gould [11] showed that $\log I$ versus $1/T$ were straight lines for a given sample, when extrapolated to negative values of $1/T$, will intersect at a common point whose coordinates are

$$\log I = \left(\frac{e^2\mu w N_C N_t A}{\varepsilon\varepsilon_0}\right), \quad 1/T = -1/T_t. \tag{13}$$

The slopes of the lines are given by

$$\frac{d(\log I)}{d(1/T)} = T_t \log\left(\frac{\varepsilon\varepsilon_0 U}{ew^2N_t}\right), \tag{14}$$

which means that the slope is dependent on the measuring voltage. Therefore the lines are not parallel but are converging in the direction of higher temperatures and, extrapolated, will meet at a common intersection point. The intercept on the $\log I$ axis ($\log I_0$) is given by

$$\log I_0 = \log(e\mu N_C U/w). \tag{15}$$

I_0 represents the current at infinite temperature ($1/T = 0$), and is a theoretical abstraction, but is given by the constant b in the equation for the line $\log I = a(1/T) + b$ for $1/T = 0$. Using the set of Eqs. (13)–(15), the main parameters μ, N_t and T_t may be obtained.

4. Results and discussion

4.1. Influence of gel film on oxide growth rate

From Table 2, it follows that the thickness of the oxide under the protecting gel film was lower by 16.5% for both kinds of zirconium alloys after 21 days of oxidation time. After 42 days of oxidation the protecting effect was 8.9% in the Zr1Nb sample, whereas in Zry-4S it was 18.5% which, with regards to the different gel film thickness, is practically the same effect as found in the 21 days samples. It is surprising that in the Zry-4S samples the oxide thickness remains almost unchanged, although the oxidation time increased twice. However, this result was not confirmed for further samples.

4.2. Relative permittivity

The diameter of the painted silver electrode, not being exactly circular, was estimated by means of a slide rule with an error of ±0.1 mm, and the capacitance was measured after annealing at 180 °C in air. The extremely low value of the relative permittivity is hard to explain. It can be seen that the added gel influences the permittivity of the double layers only by about 10% for both alloys, and the samples of Zr1Nb have higher values by about 35% than those of Zry-4S. It is interesting to note that the samples of Zr1Nb have quite a normal permittivity of about 20, whereas with half the oxidizing time they had only half this value. The samples of Zry-4S had a far less increase of the permittivity (from about 6 to 9), but remained at less than half of the normal bulk value. The main result is that the permittivity of the gel film does not differ substantially from the value of the oxide and therefore does not influence markedly the permittivity of the double layer (Table 3).

Table 3
Relative permittivity of the samples oxidized 21 and 42 days

Sample (21 days)	Gel	w (μm)	ε_r[a]	Sample (42 days)	Gel	w (μm)	ε_r[a]
T-Zr1Nb-1	Gel	4.02	11.3	T-Zr1Nb-2	Gel	4.97	18.5
Zr1Nb-1	–	2.8	9.8	Zr1Nb-2	–	3.27	22
T-Zry-4S-1	Gel	3.26	7.0	T-Zry-4S-2	Gel	2.81	11.3
Zry-4S-1	–	1.78	6.6	Zry-4S-2	–	1.84	8.2
T-41	Gel	1.5	10.0 (single gel film on Zr1Nb, without oxidation)				

[a] Error 10%.

4.3. Short-circuit current and open-circuit voltage

Measurement of the short-circuit current I_0 and the open-circuit voltage U_0 as function of slowly rising temperature showed the current to increase exponentially, while the open-circuit voltage grew linearly, starting at about 60 °C. Below this temperature neither U_0 nor I_0 could be observed (the open-circuit voltage was assessed by compensation of the short-circuit current, with a precision of 0.1 pA). All samples of Zr1Nb, with and without gel film, showed a similar behaviour with a rate of about 2 mV/°C, reaching 200 up to 300 mV at the maximum temperature of 180 °C. The flowing diffusion current develops U_0 as the voltage drop across the resistance of the oxide layer.

The samples Zry-4S had an especially low short-circuit current, due to high resistivity and a very low open-circuit voltage. A summary of the properties is given in Table 4.

4.4. Temperature dependence of the I–V characteristics, samples oxidized 21 days

The measurement of the positive branch of the I–V characteristics at constant temperatures was the main source of information. To show the procedure of assessing the transport parameters, e.g. of sample T-Zr1Nb-1 with gel, oxidation time 21 days, the positive branches of the I–V characteristics are presented in Fig. 1 in half-volt steps with 20 °C temperature increments. At zero applied voltage, and temperatures above 80 °C, zero-currents could be observed. In Table 5, the coefficients a, b, c of the fitted second order polynomials according to Eq. (1) are cited, together with the values of resistivity, mobility and free carrier concentration, using Eqs. (2)–(6) for computation. The temperature dependence of the resistivity of Zr1Nb-1 without gel was found to be similar to the sample with gel. In both

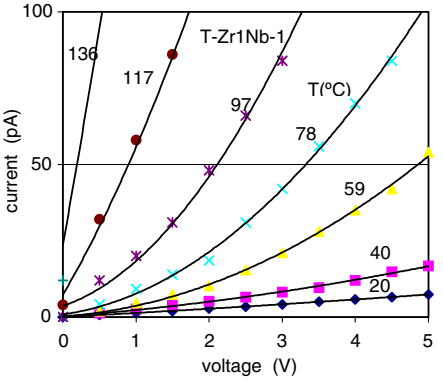

Fig. 1. Typical example of measurement of I/V characteristics (positive branches only) at constant temperatures, T-Zr1Nb-1, (with gel, oxidized 21 days), 20 °C steps, curves fitted to second order polynomial (see Table 5).

Table 4
Temperature dependence of the open-circuit voltage U_0 of the samples

Sample	t_{ox} (days)	Gel	dU_0/dT (mV/°C)	U_0(max) (mV)	At T (°C)	E (eV)
T-Zr1Nb-1	21	With gel	2.2	250	180	1.03
Zr1Nb-1	21	–	1.7	190	180	1.05
T-Zry-4S-1	21	With gel	–	–		
Zry-4S	21	–	1.3	40	130	–
T-Zr1Nb-2	42	With gel	0.14	20	170	0.43
Zr1Nb-2	42	–	2.5	300	180	0.63
T-Zry-4S-2	42	With gel	0.06 (3)	8 (60)	150 (195)[a]	0.83
Zry-4S-2	42	–	1.1	120	160	–

[a] Higher U_0 at 190 °C.

Table 5
T-Zr1Nb-1, data of $I = aU^2 + bU + c$ from Fig. 1 to compute ρ, μ, $n = f(T)$

T (°C)	a (pA/V^2)	b (pA/V)	c (pA)	R^2	ρ (Ω cm)	μ (cm^2/V s)	n (cm^{-3})
20	0.0429	1.2546	0.0699	0.9996	5.1×10^{13}	7.7×10^{-11}	1.6×10^{15}
40	0.2886	1.8571	0.1867	0.9962	3.6×10^{13}	5.2×10^{-10}	3.5×10^{14}
59	1.7492	1.7486	0.214	0.9979	3.6×10^{13}	3.1×10^{-9}	6.6×10^{13}
78	3.4289	3.3846	0.8902	0.9986	1.8×10^{13}	6.2×10^{-9}	5.1×10^{13}
97	6.5268	8.166	3.6573	0.999	7.7×10^{12}	1.2×10^{-8}	1.5×10^{14}
117	7.3287	41.029	7.3007	0.999	1.5×10^{12}	1.3×10^{-8}	3.2×10^{14}
136	16.298	133.49	23.664	0.999	4.7×10^{11}	2.9×10^{-8}	4.6×10^{14}

cases the slope of the logarithm of the resistivity is practically the same, 1.03 eV and 1.05 eV, respectively. As also the values of the resistivity are nearly equal, the gel film can be considered to have similar properties as the underneath growing oxide layer.

The currents, taken from the measured I–V characteristics of the sample T-Zr1Nb-1 in Fig 1, can be arranged as temperature functions of the form $\log I = f(1/T)_U$ with the voltage as parameter. The formed parallel straight lines shown in Fig. 2 indicate according to [10] the existence of only one kind of traps lying at a single energy level below the lower edge of the conduction band.

The most important result is the finding that the gel film did not markedly influence the properties of the growing oxide layer of Zr1Nb with the exception of retarding the growth.

Measurements at constant temperatures of I–V characteristics of the gel film of 1.5 μm thickness deposited on Zr1Nb without oxidation gave similar results as the measurement of the oxide layer of Zr1Nb alone. The logarithm of the current at constant voltages as functions of the reciprocal absolute temperature, shown in Fig. 3, gave parallel straight lines [10] indicating only one kind of traps at a single energy level at 1.08 eV, similar to Zr11Nb-1 alone, thus supporting the similarity of the gel film and of the oxide on Zr1Nb. Also the activation energy of oxide and gel film is nearly the same, 1.05, and 1.08 eV, respectively.

Contrary to Zr1Nb, the samples of Zry-4S had oxide layers quite different from the gel film. In this case we have a double layer of a gel film and, underneath, a different growing oxide layer. Assuming no interaction between both layers the resulting resistance R of their combination should be the sum of the resistances of the constituents of area A and, knowing their thickness and temperature dependent resistivities, can be computed,

$$R = R_{ox} + R_{gel} = (\rho_{ox} w_{ox} + \rho_{gel} w_{gel})/A. \quad (16)$$

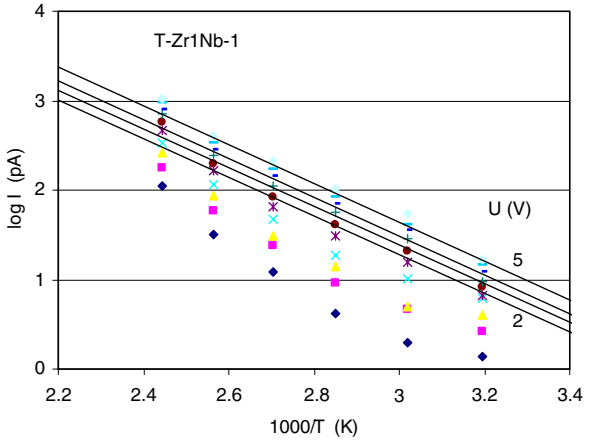

Fig. 2. Data of Fig. 1 arranged in the form of $\log I = f(1/T)_U$ to show the temperature dependence of the current at constant voltages (0.5 V steps); at voltages over 2 V, where charge limited current prevails, parallel straight lines can be put through the measuring points, indicating a single energy trap level.

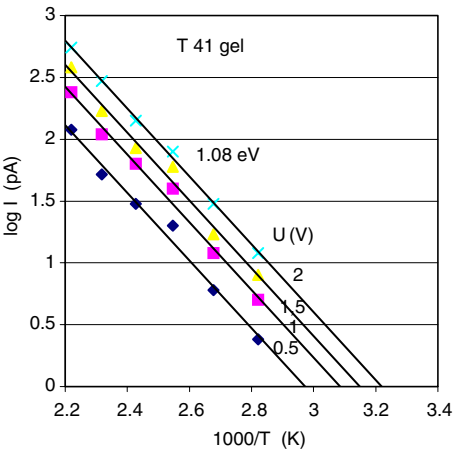

Fig. 3. Temperature dependence of $\log I$ at constant voltage (0.5 V steps) of singe gel film T-41 gel; parallel straight lines indicate a single energy trap level.

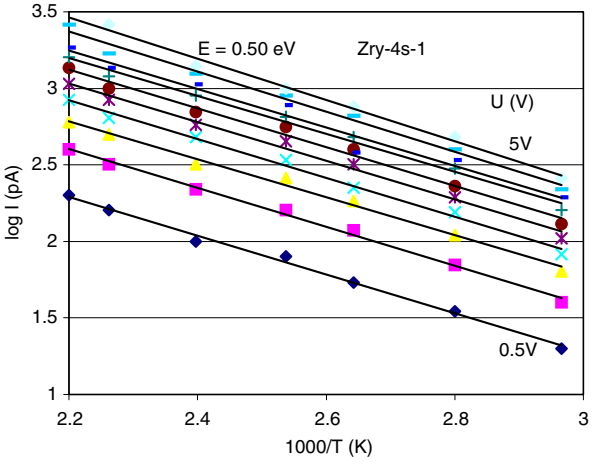

Fig. 4. Temperature dependence of current at constant voltages on Zry-4S-1, steps 0.5 V, parallel straight lines, traps on a single energy level.

The temperature dependence of the current at constant voltages of the sample Zry-4S-1, $\log I = f(1/T)_U$, is shown in Fig. 4, the straight lines indicate a single trap level at 0.5 eV. But on the sample T-Zry-4S-1, shown in Fig. 5, there is a protecting gel film forming a double layer, and the straight lines put through the measuring points are converging instead of being parallel, as in the sample without a gel film. The resistance of its components can be computed using data of Figs. 3 and 4 and their sum be compared with the resistance of the layer of T-Zry-4S-1 in Fig. 6. The directly measured resistance of the double layer is somewhat higher than

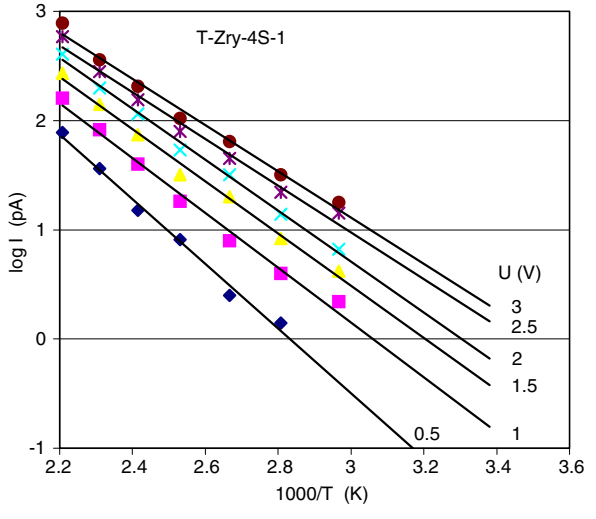

Fig. 5. Temperature dependence of current at constant voltages (0.5 V steps) of T-Zry-4S-1, showing converging straight lines.

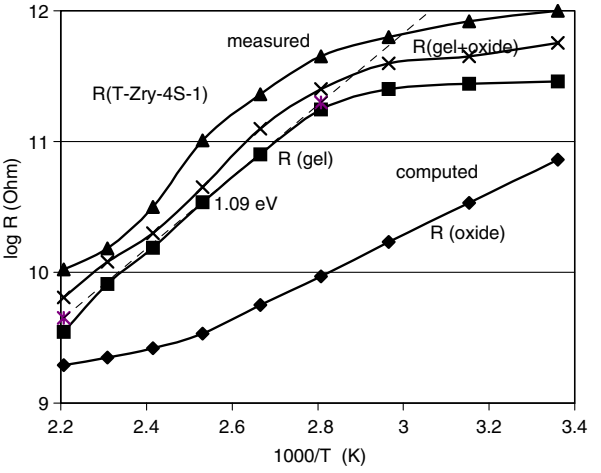

Fig. 6. Comparison of the measured and computed temperature dependent resistances of the double layer of T-Zry-4S-1, on top is the measured resistance of the double layer, below the sum $R_{(\text{gel + oxide})}$ with the computed resistances of the constituents.

the sum of the computed resistances of the oxide part and of the gel part, but with the same trend. The difference could be taken as indication of possible interaction between gel and oxide layer.

The oxide layer and the gel film in the double layer of T-Zry-4S-1 have different, but single energy trap levels, expressed as parallel straight lines with different slopes, as can be seen in Figs. 3 and 4, but acting together in the double layer, the straight lines of $\log I = f(1/T)_U$ in Fig. 5 are not parallel. With rising voltage the Fermi level will move upwards, beginning at the high level of over 1 eV of the traps in the gel film, thus producing the steepest lines, and at higher voltages will get nearer to the lower energy traps of 0.5 eV of the oxide layer, thus producing lines with lesser slopes. The decreasing slopes of the straight lines show how with increasing voltage U the influence of the traps with $E_{\text{gel}} = 1.08$ eV in the gel film is consecutively substituted by the influence of the traps with $E_{\text{ox}} = 0.5$ eV in the oxide layer. The extrapolated lines in Fig. 5 will intersect at a point, simulating in accordance with Gould's theory [10] an exponential energy distribution of traps. But as the intersection point lies in the positive section of the reciprocal temperature, Gould's [10] theory cannot be used to compute the trap concentration.

The influence of the gel film is also apparent in Fig. 7, where up to 85 °C the oxide layer predominates in the temperature dependence of the resistivity, producing the low activation energy, and the

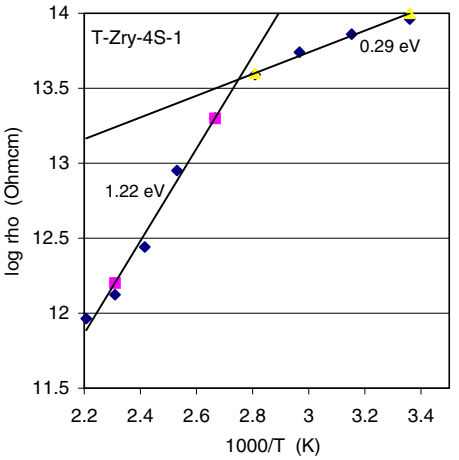

Fig. 7. Temperature dependence of the resistivity of T-Zry-4S-1, at low temperatures prevails the influence of the oxide, and at higher temperatures the higher activation energy of the gel film is activated.

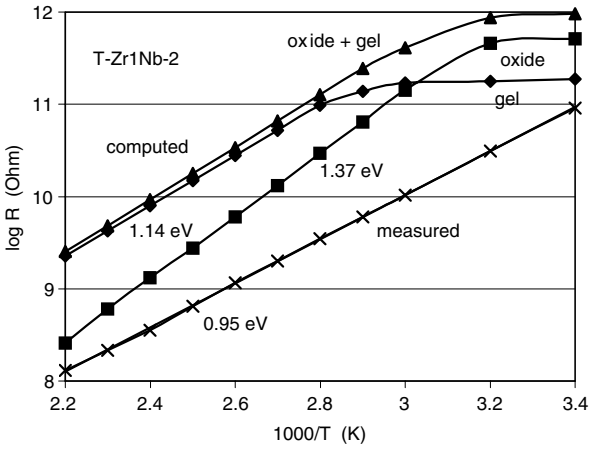

Fig. 8. Comparison of the measured and computed temperature dependent resistances of the double layer of T-Zr1Nb-2, on top is the sum of the computed resistances of the oxide layer and of the gel film, and down the measured lower resistance of the double layer.

higher energy of the gel film centers is activated at higher temperatures resulting in the high value of the observed activation energy.

4.5. Temperature dependence of the I–V characteristics, samples oxidized 42 days

The measuring procedure was the same as for the samples of the first batch. The temperature dependence of the resistivity for Zr1Nb-2 is very similar to that of the gel film, where there also is observed a sharp drop in resistivity of the same order of magnitude and a temperature independent carrier concentration. This indicates the same consistency of the gel film and of the oxide layer on Zr1Nb. It was therefore to be expected that the properties of a combination of both gel film and oxide, in the double layer of sample T-Zr1Nb-2, would also be the sum of the properties of the constituents, as had been found in the 21 days oxidized double layer of T-Zr1Nb-1. The resistance of the double layer of the sample was assessed directly by measuring the current at 0.1 V with rising and falling temperature, the rate of temperature change being about 1 °C/min. The diameter of the silver contact had to be only 1.0 mm to avoid weak spots on the surface of the layer causing shorts. But in Fig. 8 there is shown, in the lower curve, the measured resistance of the double layer and, in the upper part, the computed resistances of the oxide layer and the gel film and their sum, which is different. The main result is the finding that the measured resistance of the double layer is lower than the sum of its computed parts, which means that both constituents had been lowering their resistivity, but on the whole maintaining their activation energy. This behaviour was not apparent on the sample T-Zr1Nb-1 oxidized 21 days, possible changes being lost in the error margin. But after 42 days of oxidation the time was long enough to cause measurable changes of the gel film by interaction with the contacting oxide layer which, vice versa, was influenced by the gel film.

Afterwards the sample Zry-4S-2, clean oxide layer without a gel film, with a silver contact of 2.5 mm diameter, was measured at room temperature yielding a very high resistivity of 6.1×10^{14} Ω cm. Gradually rising temperature produced an extremely low short-circuit current of 2.3 pA at 140 °C, and exponential increase till over 160 °C. The open-circuit voltage started at 70 °C with a linear slope of 1.15 mV/°C, reaching 120 mV at 160 °C, and then rising faster. The resistivity remained nearly unchanged up to 60 °C, and then dropped with an activation energy of 0.94 eV. Although the temperature independent carrier concentration was with 2×10^{15} cm^{-3} unusually high, the conductivity was nevertheless very low due to an extremely low mobility of 2.4×10^{-12} cm^2/V s at room temperature.

The logarithm of the current at constant voltages, taken from the measured characteristics, gives straight lines shown in Fig. 9, parallel up to 3 V, but slightly divergent for 4 and 5 V, indicating one kind of traps at a single energy level.

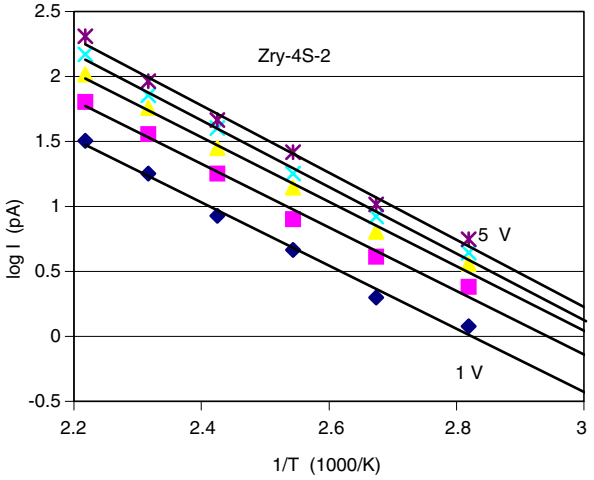

Fig. 9. Temperature dependence of $\log I$ at constant voltages on Zry-4S-2, parallel straight lines indicate traps on a single energy level.

The dissimilar properties of the Zry-4S samples, differing only in oxidation time, is hard to explain. There are marked differences, in resistivity, mobility and activation energy, as can be seen in Table 5 at the end.

The properties of the sample T-Zry-4S-2 were quite different from the sample without the gel film. The resistivity was considerably lower, the open-circuit voltage was extremely low, only 0.06 mV/°C, as well as the short-circuit current, but rising exponentially at temperatures above 160 °C.

Measurement of the I–V characteristics at constant temperatures in 20 °C steps up to 180 °C, and supported by direct measurement of the current at constant 0.1 V with continually rising temperature, gave the temperature dependence of the resistivity with the activation energy of 0.87 eV.

In Fig. 10, the measured resistance of the double layer of T-Zry-4S-2 is compared with the computed sum of the resistances of the oxide layer (data taken Zry-4S-2) and of the gel film. In consequence of the preponderance of the extremely high resistivity of the oxide layer of the comparing sample Zry-4S-2, the sum $R_{ox} + R_{gel} \cong R_{ox} \gg R_{meas}$. This indicates the existence of interaction between the gel film and the oxide layer, consisting of a very slow diffusion of active centers in both directions, and resulting in a pronounced drop of resistivity of the growing oxide film, as well as a lowering of the resistivity of the gel film. The abnormally low resistivity of the double layer was confirmed by subsequent measurement of the resistance of several other contacts with different areas A.

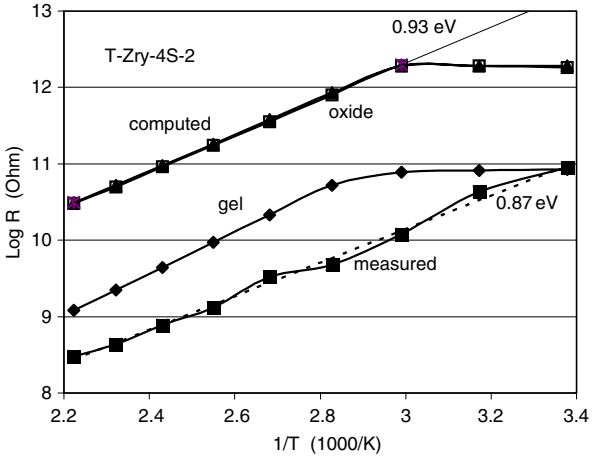

Fig. 10. Comparison of the measured and computed temperature dependent resistances of the double layer of T-Zry-4S-2. On top is the sum of the computed resistances of the oxide and of the gel film, only very little higher than the resistance of the oxide alone, in consequence of the very small resistance of the gel film. The measured resistance of the double layer is the lowest curve.

The temperature dependence of the logarithm of the currents at constant voltages ($\log I = f(1/T)_U$), data taken from the V–I characteristics, is presented in Fig. 11. The resulting straight lines are converging, but due to measuring errors do not all meet at a common intersection point. Therefore, as in the sample oxidized 21 days, the coefficients A and B of the interpolation equations $\log I = A(1/T) + B$ representing the straight lines in Fig. 11 were plotted as functions of the voltage parameter of the straight lines, and corrected values A_{cor} and B_{cor} were computed from the regression lines.

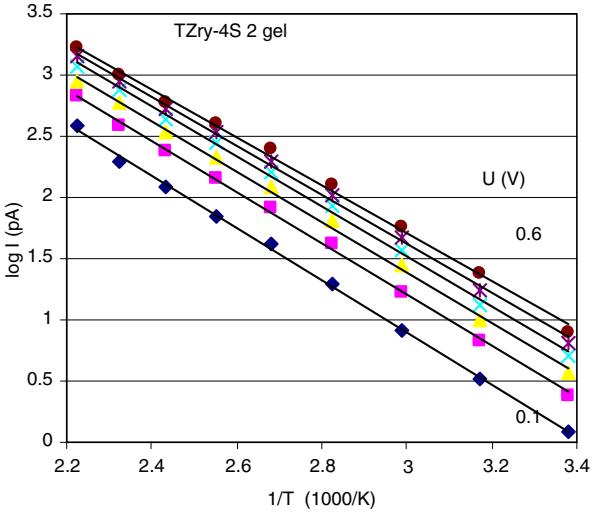

Fig. 11. Temperature dependence of $\log I$ at constant voltages on T-Zry-4S-2 giving converging straight lines.

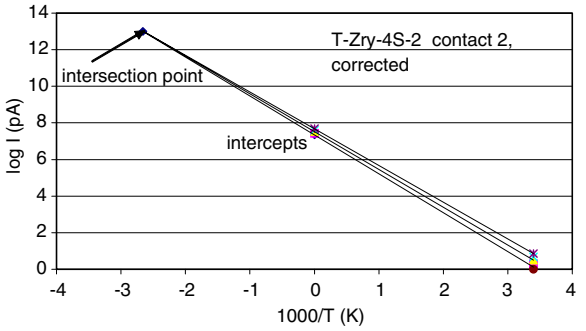

Fig. 12. Extrapolated (corrected) lines of Fig. 11 meeting at a common intersection point.

Taking two corrected lines $\log I = A_{\mathrm{cor}}(1/T) + B_{\mathrm{cor}}$, for any two voltages e.g. for 0.1 V, and 0.5 V, respectively, the solution gives the intersection point at $1000/T = -2.66$ (with a virtual temperature of $T_t = 376$ K and a current $I_t = 10$ A), as can be seen in Fig. 12. Contrary to the sample T-Zry-4S-1 with an oxidation time of only 21 days, where the intersection point was in the real temperature range where, according to Gould's theory [10] it should not be found, in this case the intersection point lies in the negative temperature range as would be expected for an exponential energy distribution of traps. Now Fig. 3 for the single gel film and also Figs. 4 and 9 for the samples of Zry-4S without gel film show parallel straight lines indicating traps on a single energy level, but together in the double layer, have converging lines characteristic of an exponential energy distribution of traps. Different kinds of traps in the gel film and in the oxide layer of the Zry-4S samples can be expected to mix by interdiffusion in the double layer and thus simulate a mean trap distribution over a larger energy range resembling an exponential trap distribution.

An extrapolated straight line with voltage U at $1/T = 0$ has an interception point with the $\log I$ axis, defining a current in the form of $\log I_0 = B_{\mathrm{cor}}$. Choosing $U = 0.5$ V, the responding value of B_{cor} specifies the current $I_0 = 4.8 \times 10^{-5}$ A and using Eq. (15), with an assumed value of the density of states of $N_C = 1 \times 10^{21}$ cm^{-3}, the mobility appears to be 3.4×10^{-9} cm^2/V s, which is of the right order of magnitude.

The I–V characteristic at room temperature can be represented by the interpolation formula

$$I(\mathrm{pA}) = 3.5714U^2 + 11.07U + 0.0286,$$ which yields $\rho = 1.48 \times 10^{13}\ \Omega$ cm, $\mu = 7.5 \times 10^{-10}$ cm^2/V s and the concentration of free carriers $n = 5.1 \times 10^{14}$ cm^{-3}.

The characteristic voltage, where ohmic and space-charge limited currents are equal, is $U_{\mathrm{ch}} = b/a = 3.1$ V, giving with Eq. (5) $n = 2.6 \times 10^{14}$ cm^{-3}. Comparing $\mu = 3.4 \times 10^{-9}$ cm^{-3} and $n = 1.3 \times 10^{14}$ cm^{-3}, taken from the characteristics, is of the same order of magnitude and with regards to the assumed value of the density of states of fairly good agreement. On the other hand, assuming Gould's Theory to be valid [10], the trap concentration, using Eq. (13) with $N_C = 1 \times 10^{21}$ cm^{-3}, $\mu = 3{,}4 \times 10^{-9}$ cm^2/V s, $w = 2.78 \times 10^{-4}$ cm, $A = 0.048$ cm^2 and $\varepsilon_r = 12$, would be $N_t = 9.1 \times 10^{18}$ cm^{-3}. This result can be verified by means of Eq. (14) by comparing the slope of the straight line in Fig. 11, which is $A_{\mathrm{cor}} = -2.0$ at $U = 0.5$ V, with the right hand side of Eq. (14), being 376 $\log 4.7 \times 10^{-6} = -2000$. This is equal to the derivative -2.0 on the left hand side of Eq. (14) by the factor 1000, respecting the inverse absolute temperature expressed in 1000/K, and supports the correctness of the computation.

The density of states N_C can be computed by means of Eq. (15), using the intercept of the straight line for 0.5 V with the y-axis in Fig. 12, being at 4.8×10^{-5} A. Taking the influence of the measuring errors on the assessment of the intercept of the straight lines in Fig. 12 into account, the result, $N_C = 1 \times 10^{20}$ cm^{-3}, can be considered to be sufficiently near to the assumed density of states of 1×10^{21} cm^{-3}.

The formation of converging straight lines in Fig. 12 could be understood as the action of traps simulating an exponential energy distribution, which had been created by interdiffusion of two different kinds of traps from the gel film and the oxide layer by prolonged oxidation time. As there is no real exponential trap distribution, Gould's theory [10] is not applicable and the seemingly good results, achieved by using the intersection point of Fig. 12, are fortuitous.

5. Conclusions

The main results can be stated as follows:

(a) The gel film protects the metal surface to a certain degree, retarding but not inhibiting the growth of an underlaying oxide layer.

(b) The gel film and the oxide layer form a double layer system, where different active centers may mix by interdiffusion, thus changing the properties of both gel film and oxide layer after extended oxidation times.
(c) The oxides of the *Zr1Nb* samples had similar properties as the overlying gel film, both had practically the same resistivity, activation energy, mobility and free carrier concentration. The double layer, after the shorter oxidation time of 21 days, retains these parameters. The gel film and the oxide contain no dopant atoms (niobium does not form active centers) and therefore there are only defects of the ZrO_2 lattice creating traps at a single energy level below the conduction band edge. This is supported by the voltage independent slope of the straight lines of $\log I = f(1/T)_U$.
(d) Longer oxidation time (42 days) increases the resistivity of the oxide by lowering the mobility at nearly unchanged carrier concentration if left alone, but together with the gel film in the double layer the resistivity decreases. The resistance of the double layer is less than the sum of the resistances of the gel film part and of the oxide layer part computed from the resistivities of the constituents which means that the resistivities, of both the gel film and of the oxide layer forming the double layer, were diminished.
(e) In the *Zry-4S* samples the resistivity increased also with oxidation time and decreased in gel-protected layers. The main difference compared with the Zr1Nb samples was the appearance of converging straight lines of $\log I = f(1/T)_U$ in the gel-protected samples, although the corresponding samples of the constituents had parallel straight lines.
(f) The straight lines converging in a common intersection point indicate the existence of traps distributed over a certain energy range. This can be interpreted as the influence of different single energy trap levels in the gel film and the oxide layer. The traps can be mixed by interdiffusion in both parts of the double layer after extended oxidation time, thus giving the impression of an exponential energy trap distribution.
(g) Application of Gould's theory [10] to state the trap concentration by analysis of the converging straight lines of $\log I = f(1/T)_U$ is not permissible and seemingly good results are fortuitous.

Acknowledgements

The research part concerning the preparation of the gel films was supported by the Czech Science Foundation Project No. A VOZ30460519 and 06/04/0043. Sample preparation at UJP, Praha a.s., was supported by Grants of the Grant Agency of the Czech Republic. Financial support of the investigation of the properties of the samples by UJP, Praha a.s., is highly appreciated.

References

[1] H. Frank, J. Nucl. Mater. 340 (2005) 119.
[2] D.G. Franklin, P.M. Lang, C.M. Eucken, A.M. Garde (Eds.), Proceedings of the Ninth International Symposium on Nuclear Industry, ASTM, Philadelphia, ASTM STP 1132, 1992, p. 3.
[3] Corrosion of Zirconium Alloys in Nuclear Power Plants, IAEA-TECDOC-684, Vienna 1993.
[4] M.M.R. Howlader, K. Shiiyama, C. Kinashita, M. Kutsuwada, M. Inagaki, J. Nucl. Mater. 253 (1998) 491.
[5] M. Inagaki, M. Kanno, H. Maki, ASTM-STP 1132 (1992) 437.
[6] A. Charlesby, Acta Metall. 1 (1953) 348.
[7] N.F. Mott, R.W. Guerney, Electronic Processes in Ionic Crystals, Clarendon, Oxford, 1940.
[8] A. Rose, Phys. Rev. 97 (1955).
[9] M.A. Lampert, Rep. Prog. Phys. 27 (1964) 329.
[10] R.D. Gould, M.S. Rahman, J. Phys. D: Appl. Phys. 14 (1981) 79.
[11] R.D. Gould, J. Appl. Phys. 53 (1982) 3353.
[12] R. Brenier, A. Gagnaire, Thin Solid Films 392 (2001) 142.
[13] R. Brenier, C. Urlacher, J. Mugnier, M. Brunel, Thin Solid Films 338 (1999) 136.